DOI: 10.2478/ncr-2018-0009

ISSN online 2545-2819

ISSN print 0800-6377

Received: March 15, 2018

Revision received: May 29, 2018

Accepted: May 29, 2018

Towards the Understanding of the pH Dependency of the Chloride Binding of Portland Cement Pastes

Alisa Machner
Researcher, NTNU
Department of Structural Engineering
Richard Birkelandsvei 1A
7491 Trondheim
alisa.machner@ntnu.no

Petter Hemstad
MSc Student, NTNU
Department of Materials Science and Engineering
Alfred Getz vei 2
7491 Trondheim
petter@hemstad.net

Klaartje De Weerdt
Førsteamanuensis, NTNU
Department of Structural Engineering
Richard Birkelandsvei 1A
7491 Trondheim
klaartje.d.weerdt@ntnu.no

ABSTRACT

Hydrated Portland cement paste exposed to a NaCl solution was acidified by adding HCl in small steps, gradually lowering the pH. The chloride binding of the cement paste changed as a function of the pH. For the range of pH from 13.2 to 12.2, decreasing pH resulted in a considerable increase in the chloride binding. At a pH of 11, the cement paste showed almost no chloride binding. In order to explain the changes in chloride binding upon lowering the pH, the phase assemblage was investigated with SEM-EDS, TGA and XRD and compared to a thermodynamic modelling.

Key words: chloride binding, pH, C-S-H, thermodynamic modelling, leaching

1. INTRODUCTION

One of the major deterioration mechanisms of reinforced concrete structures, which can limit their service life, is chloride induced corrosion of the reinforcement steel. As chlorides diffuse into the concrete structure from external sources such as sea water or de-icing salts, the chloride concentration at the reinforcement will eventually increase. When a critical chloride concentration is reached in the proximity of the reinforcement, pitting corrosion of the steel may be initiated. The time until the critical concentration at the steel surface is reached is therefore generally used as a limit state for the service life of a reinforced concrete structure.

Service life prediction models commonly predict the chloride ingress profiles using Fick's law [1,2], which describes diffusion caused by a concentration gradient [3]. Ions, such as chlorides, dissolved in the pore solution, will always move from a high concentration to a lower concentration in the pore solution unless opposed by other forces. Figure 1 shows experimentally obtained chloride profiles (solid lines) of Portland cement mortar samples exposed to sea water, and fitted curves using the error function solution of Fick's law (dashed lines) [4]. With increasing distance from the surface, the chloride content in the mortar decreases according to Fick's law. However, with increasing exposure time, the outermost sections show a lower chloride content than the fitted solution of Fick's law, and show a peak before decreasing with increasing depth from the surface.

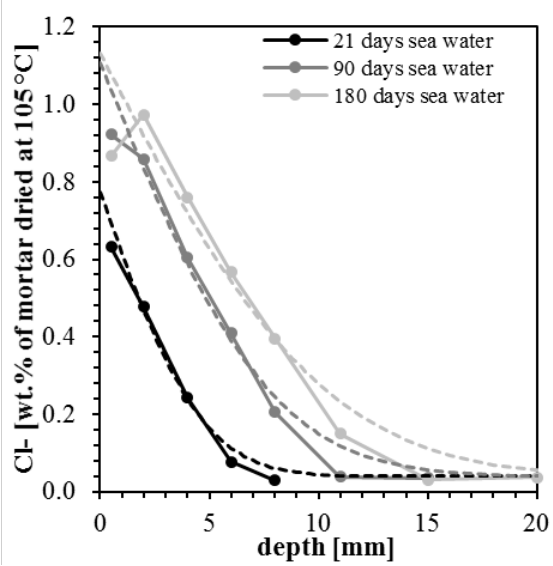

Figure 1 - Chloride profiles experimentally obtained on Portland cement mortars submerged in sea water for 21, 90, and 180 days (solid lines) and fitted to the error function solution of Fick's law (dashed lines) (adapted from [4]).

Similar peaking behaviour in chloride profiles have also been reported elsewhere [5–8]. Current service life models ignore the outer sections and only use the parts of the chloride profile that fits the mathematical model [2]. Our hypothesis is that we can capture this peaking behaviour if we are able to take into account leaching in the models.

When concrete is exposed to sea water there are several phase changes that occur with varying depths of penetration [5]. Due to the presence of $Ca(OH)_2$ and the alkali metal content in hydrated cement paste, the pore solution is highly alkaline, with a pH of 13 or even higher [9]. Constant exposure to sea water of near neutral pH will reduce the pH of the pore solution. The phase assemblage in the cement paste will change both because the pH is lowered, and because of ingress of ions from the sea water.

In the cement paste, chlorides are bound either chemically, by the formation of chloride-containing AFm phases, such as Friedel's salt ($3CaO{\cdot}Al_2O_3{\cdot}CaCl_2{\cdot}10H_2O$), or physically, by their accumulation in the diffuse layer of the C-S-H phase [10]. Consequently, changes in the phase assemblage of the cement paste with regards to Friedel's salt or the C-S-H phase caused by the exposure of concrete structures to sea water might be the reason for the deviation of the chloride profiles experimentally obtained from Fick's law.

Changing pH influences both the chemical and physical binding of chlorides. Roberts [11] showed that lowering the pH would slightly increase the stability of Friedel's salt, thus increasing the chemical chloride binding of the cement. Lowering the pH too far would however decrease its stability and lead to reduced binding [12,13]. Since OH^- and Cl^- both accumulate in the diffuse layer of the C-S-H, they can be considered as competitively adsorbing ions. Reducing the pH would reduce the competition from OH^-, thereby increasing the apparent adsorption of Cl^- in the diffuse layer [14]. Small decreases in the pH were reported to increase the chloride binding of the cement paste [14,15]. However, this was done by introducing chlorides in the mixing water, which will affect the microstructure of hydrated concrete. Because of this effect, studies using admixed chlorides might not be representative for external chloride ingress and binding in concrete. The exposure of cement pastes to $CaCl_2$ solutions has also been reported to be accompanied by a decrease in the pH of the pore solution and an increase in chloride binding [14,16–19]. However, no previous studies have systematically investigated how pH affects chloride binding for chlorides introduced after hydration.

The focus of this study was therefore to develop a method for studying chloride binding for hydrated cement pastes exposed to chlorides and systematically lowering the pH. Well-hydrated cement pastes of ordinary Portland cement (OPC) were exposed to a NaCl-solution. HCl was then added to lower pH without adding other types of ions not already present in the system. First, a relationship between volumes of added acid and pH in the pore solution was established. This relationship was used to determine how much acid is required to reach specific pH-levels. The combination of changes in the phase assemblage and lowering of the pH in the pore solution upon acid addition is referred to as leaching in this study. The second part of this study consists of acidifying five cement paste samples to targeted levels of pH and determine how the acidification affects the chloride binding. The effects of artificial leaching with HCl on the phase assemblage were studied, to explain the mechanisms causing changes in chloride binding.

2. MATERIALS AND METHODS

2.1 Materials and sample preparation

In this study, Portland cement pastes were investigated, prepared with an ordinary Portland cement (OPC) supplied by Norcem AS, to which only natural gypsum was added during grinding. Table 1 shows the chemical composition of the Portland cement used determined with

X-ray fluorescence (XRF). The Portland cement used had a Blaine specific surface of 416 m^2/kg.

Table 1 - Chemical composition of the Portland cement (OPC) used determined with XRF [wt. %].

	SiO_2	Al_2O_3	TiO_2	MnO	Fe_2O_3	CaO	MgO	K_2O	Na_2O	SO_3	P_2O_5
OPC	19.91	5.15	0.28	0.06	3.42	62.73	2.34	1.09	0.48	3.16	0.11

The cement paste was prepared in 4 batches of 540 g with a w/b ratio of 0.5 in a high-shear mixer (Braun MR5550CA). The pastes were mixed for 30 s, left to rest for 5 min and mixed again for 60 s. The paste was cast in several plastic bottles (125 mL) and sealed with a lid and parafilm. The tubes were stored up to their bottle necks in water in sealed boxes at 60°C. To maximize hydration and thus minimize any continued hydration during exposure, the samples were ground and rehydrated after 3 months of curing. They were crushed in a jaw crusher and sieved through a 1 mm sieve. Remaining particles were crushed further in a rotating disc mill until they also passed the sieve. After crushing, the samples were put in 1 L polypropylene bottles with additional 30wt% of water. The bottles were then sealed with lids and parafilm, and stored for another 4 months at 60°C. After this final curing at 60°C, the bottles were stored at 20°C for 13 months before chloride exposure. The exposure was also performed at 20°C.

2.2 Exposure of the samples to NaCl and HCl

For the exposure, 15 g of the well-hydrated cement paste, which had a homogenous moist-sand appearance, was weighed into 50 mL centrifuge tubes, to which 20 mL of NaCl solution (1.5 mol/L) was added using a volumetric pipette. The 1.5 mol/L NaCl solution was prepared with deionized water and laboratory-grade NaCl (supplied by Merck). The tubes were then closed with lids and parafilm, and thoroughly shaken to mix the liquid and the solid. They were then left for two weeks at 20 °C to reach equilibrium, while being shaken once per week to ensure full exposure.

After reaching equilibrium with the NaCl solution, one sample (OPC-22.5, see Table 2) was used to establish the relationship between the volume of added acid and the resulting pH of the pore solution. For this 4 mol/L HCl was added in steps until the sample tube was filled. The acid was added in small steps to avoid uneven dissolution of the hydrated cement paste. In addition, the samples were centrifuged and the acid was added to the supernatant to avoid direct contact between the acid and the solids. The acid was first added in 10 steps of 0.25 mL, then 4 steps of 0.5 mL, 3 steps of 1 mL, then in 8 steps of 2 mL until the sample tube was filled. The final volume of acid added was 22.5 mL. The pH of the sample was measured after 10-15 minutes and after 1-3 days of each addition step ("instant pH" and "pH at EQ" respectively in Figure 3).

To one sample tube no HCl was added (OPC-0, see Table 2). This sample was used as a reference. To the other tubes of the prepared and equilibrated samples, various amounts of 4 mol/L HCl (0.5, 2.5, 5, and 17 mL) were added in small steps (12 steps of 0.25 mL, then 2 steps of 0.5 mL, then 1 step of 1 mL, then 6 steps of 2 mL) to reach the target pH in the pore solution (see Table 2). The additions were stopped after the target acid volume was reached in the various samples. After each addition, the samples were shaken and left to rest until the next acid addition. Acid was added each workday, leading to a minimum resting time of 1 day and a maximum of 3 days. After having the full amount of acid added, the samples were stored at 20°C for two weeks, while they were all shaken once per week.

Table 2: Overview of the various exposed samples in this study.

Sample name	Cement paste [g]	1.5 mol/L NaCl [mL]	4 mol/L HCl [mL]
OPC-0 (Reference)	15.00 ± 0.01	20	-
OPC-0.5	15.00 ± 0.01	20	0.5
OPC-2.5	15.00 ± 0.01	20	2.5
OPC-5	15.00 ± 0.01	20	5
OPC-17	15.00 ± 0.01	20	17
OPC-22.5 (pH development)	15.00 ± 0.01	20	22.5

2.3 Analyses after exposure

Analyses of the liquid

The liquid phase of the samples was investigated 2 weeks after exposure to the NaCl solution (OPC-0) or 2 weeks after the full amount of acid had been added (OPC-0.5 – OPC-17).

The chloride concentration in the liquid phase was determined by potentiometric titration with a Titrando 905 titrator from Metrohm using 0.1 mol/L $AgNO_3$ solution (Titrisol, supplied by Merck). A known volume (0.2–1 mL, depending on the chloride concentration of the exposure solution) of the supernatant was pipetted into a measurement beaker with 1 mL of HNO_3 (65% supplied by Merck, and diluted 1:10), 2.5 mL of 0.2% polyvinyl alcohol (supplied by Merck, 2 g was dissolved in 1 L deionized water), and approx. 20 mL of deionized water.

The actual concentration of free chlorides present before binding ($C_{Cl,free}$) was calculated using Eq. (1) according to [20]:

$$C_{Cl,free} = \frac{(C_{NaCl} \cdot V_{NaCl}) + (C_{HCl} \cdot V_{HCl})}{V_{H_2O} + V_{NaCl} + V_{HCl}} \quad (1)$$

where C_{NaCl} is the concentration of chlorides in the NaCl solution, which was measured with potentiometric titration prior to exposure; C_{HCl} is the concentration of the acid used (4 mol/L); V_{NaCl} is the volume of NaCl solution added to the samples (20 mL); V_{HCl} is the volume of acid added to the various samples (0, 0.5, 2.5, 5, 17 mL); V_{H2O} is the volume of free water (in g) per 15 g of the well-hydrated hydrated cement paste before exposure, and was assumed to be equal to m_{H2O} (4.6 g per 15 g of well-hydrated cement paste), which was determined by the weight loss of the unexposed well-hydrated cement pastes after drying at 40°C in a TGA until constant weight.

During the exposure of cement pastes, chlorides from the solution are bound by the hydrates of the cement paste. The chloride concentration in the solution will therefore decrease until equilibrium between the solid and the liquid phase is established. The amount of bound chlorides ($N_{Cl,bound}$) can be calculated as mg/g cement paste dried at 40°C using Eq. (2), according to [20]:

$$N_{Cl,bound} = \frac{M_{Cl} \cdot \left(C_{Cl,free} - C_{Cl,eq}\right) \cdot (V_{H_2O} + V_{NaCl} + V_{HCl})}{m_{sample} - m_{H_2O}} \quad (2)$$

where $C_{Cl,free}$ is the actual concentration of free chlorides present at the beginning of the exposure (in mol/L), which can be calculated using Eq. (1); $C_{Cl,eq}$ is the chloride concentration of the supernatant measured at equilibrium (in mol/L); M_{Cl} is the molar mass of chlorine (35.453 g/mol); m_{sample} is the mass of the sample added to the centrifuge tube (15 g); and m_{H2O} is the mass of free water (in g) per 15 g of hydrated cement paste.

After determining the amount of free chlorides, the pH of the liquid phase was measured using a 6.0255.100 Profitrode from Metrohm in the laboratory at 20°C. Before measuring the pH, the sample was centrifuged at 4000 rpm for 2 minutes and 30 seconds. 2 mL of the supernatant was pipetted into 15 mL centrifuge tubes, in which the pH was measured. The electrode was calibrated each day before the measurements using buffer solutions of pH 7, 10 and 13. After each measurement, the remaining supernatant was poured back into the sample.

The concentrations of Ca, Cl, K, Na and S and in the solution were determined by a Thermo Scientific Element 2 ICP-MS. 150 µl of the supernatant was acidified with 104 µl 65 % HNO_3. This mixture was then diluted to 15 ml with deionized water, to reach a HNO_3-contentration of 0.1 mol/L in the samples.

Analyses of the solid

After concluding the investigations of the liquid phase, the phase assemblage in the Portland cement pastes was investigated. For that approximately 3-5 g of cement pastes was taken out from the centrifuge tubes and was placed in 125 mL plastic bottles with 100 mL isopropanol. The bottles were shaken for 30 seconds before resting for 5 minutes. After resting, the liquid was decanted and another 100 mL isopropanol was added. The bottles were again shaken for 30 seconds and left to rest for 5 minutes, before the contents were poured into a vacuum filtration unit. The isopropanol was filtrated off, and 20 mL petroleum ether was added. The petroleum ether and solids were stirred with a glass rod for 30 seconds before resting for 5 minutes. Afterwards, the petroleum ether was filtrated off using a vacuum filtration unit, and the samples were dried in a desiccator overnight under a slight vacuum (-0.2 bar) applied using a water pump. A part of the dried samples were ground to a particle size <63 µm and then analysed with TGA or XRD. The rest of each of the dried samples was not ground and used for SEM-EDS investigations.

Thermogravimetric analysis (TGA) was used to determine the free water content in the well-hydrated samples before exposure to a NaCl solution, and to investigate the phase assemblage in the samples, which were exposed to only NaCl or NaCl and various amounts of HCl. For all TG analyses, approximately 150 mg of the solids were placed in 600 µl alumina crucibles and analysed in a Mettler Toledo TGA/DSC3+ device. To determine the free water content of the cement paste prior exposure, non-solvent exchanged paste was dried at 40°C until constant weight (10 hours) while purging with N_2 at 50 mL/min. The weight loss was normalized to the initial sample mass, giving the free water content of the cement paste. The solvent exchanged, dried, and ground samples were heated from 40 to 900°C with a heating rate of 10°C/min while purging with N_2 at 50 mL/min. The decomposition of specific phases can be detected as a weight loss in specific temperature intervals. This was used to identify various hydration phases as suggested by Lothenbach et al. [21]. The first weight loss peak at around 100°C is related to the ettringite (Et) decomposition and the beginning of the dehydroxylation of the C-S-H phase. C-S-H decomposes gradually between 40°C and 600°C and appears as a polynomial baseline

under the other peaks. AFm phases such as monosulphate (Ms), monocarbonate (Mc), and Friedel's salt (Fs) shows typically two mass loss events, the first one between 150 and 200°C and the second between 250 and 400°C. Hydrotalcite (Ht) typically also causes a decomposition peak in the DTG signal around 350°C. The subsequent sharp peak between approx. 400°C and 550°C is related to the decomposition of portlandite (CH). Above 550°C, carbonates decompose and emit CO_2.

The dried powders were also analysed using X-ray diffraction (XRD) to confirm phase changes. Approximately 0.5 g of the powders were placed in the sample holders by front loading. We used a Bruker AXS D8 Focus with a Lynxeye detector, operating at 40 kV and 40 mA with a CuKα radiation source (wavelength 1.54 Å). The samples were measured between 5° 2θ to 55° 2θ, with a step size of 0.01° 2θ, and a sampling time per step of 0.5 s.

The samples to be investigated with scanning electron microscopy (SEM) were cast in epoxy, polished and carbon-coated. A Hitachi S-3400N electron microscope equipped with an energy dispersive spectrometer (EDS) from Oxford Instruments was used. BSE images and EDS-maps of all samples were captured, in addition to 100 EDS point-scans of the cement paste matrix per sample. The SEM was operated at an accelerating voltage of 15 keV and a probe current of 70 µA, a working distance of 5 mm for taking the BSE images, and a working distance of 10 mm for operating the EDS.

Thermodynamic modelling

The Gibbs free energy minimization software for Geochemical Modelling [22–24], was used to model the phase assemblage, the pH, and the composition of the liquid phase at equilibrium with increasing amounts of HCl (4 mol/L) added at 20°C. The thermodynamic data from the PSI-GEMS database were supplemented with a cement-specific database (CEMDATA14 database) [25], which includes solubility products of the solids relevant for cementitious materials. For the C-S-H phase, the CSHQ model proposed by Kulik was used [26]. For the model, TiO_2, MnO, MgO, and P_2O_5 and C_4AF were assumed to be inert. Therefore, the amounts of TiO_2, MnO, P_2O_5 and MgO in the cement clinker determined with XRF (see Table 1) were subtracted from the composition. The amount of C_4AF was calculated with the Bogue calculation, and then subtracted from the composition. The remaining oxide composition (approx. 85%) was then normalized to 100 %. A reaction degree of 50% was assumed in the modelling. Taking into account that only 85% of the oxide composition was used as input in the model, this resulted in a total assumed reaction degree of the cement of approx. 70%. During the modelling the following phases were prevented from forming: gibbsite, kaolinite, siliceous hydrogarnet, thaumasite, hematite, magnetite, brucite and quartz. Further details on the model are provided in [27]. In the model, Friedel's salt is the only phase that is assumed to bind chlorides. The chloride binding predicted by the model was therefore calculated using the amount of Friedel's salt predicted by the model (for more details on the calculations see [27]).

3. RESULTS AND GENERAL DISCUSSION

3.1 Development of the pH with increasing amounts of acid added

First, we needed to determine the acid additions that would yield a relevant change in the pH and the phase assemblage for further investigation. As hydrated cement paste is a complex system with several pH-buffering phases, we used the thermodynamic model to predict the changes in the pH of the exposure solution and the phase assemblage upon the addition of increasing volumes of acid (HCl). The system initially consisted of 15 g moist hydrated cement paste and 20 mL of 1.5 mol/L NaCl solution. One of the limitations was the volume of exposure solution, as high volumes of exposure solution would increase the error on the determination of the bound chlorides. Preliminary simulations pointed out that HCl with a concentration of 4 mol/L would allow us to reach sufficiently low pH for a limited volume of acid added (50 mL exposure tubes).

Figure 2 shows the volume of the phases in the samples as a function of the volume of HCl (4 mol/L) added, as predicted by the thermodynamic model. The amount of portlandite is predicted to decrease linearly with increasing acid addition until it has completely dissolved at 10 mL of acid added. Once the portlandite completely dissolved, the C-S-H is predicted to start dissolving as well. The volume of ettringite remained stable until 19 mL of acid was added, after which the volume decreased steadily until it was fully removed at 21 mL acid. The amount of Friedel's salt remained nearly constant up to 15 mL acid, for higher volumes it starts dissolving until nothing is left at 17.5 mL acid. At high volumes of acid and low pH, the model predicted the formation of natrolite ($Na_2O{\cdot}Al_2O_3{\cdot}3SiO_2{\cdot}2H_2O$), gypsum ($CaSO_4{\cdot}2H_2O$) and amorphous silica ($SiO_2$).

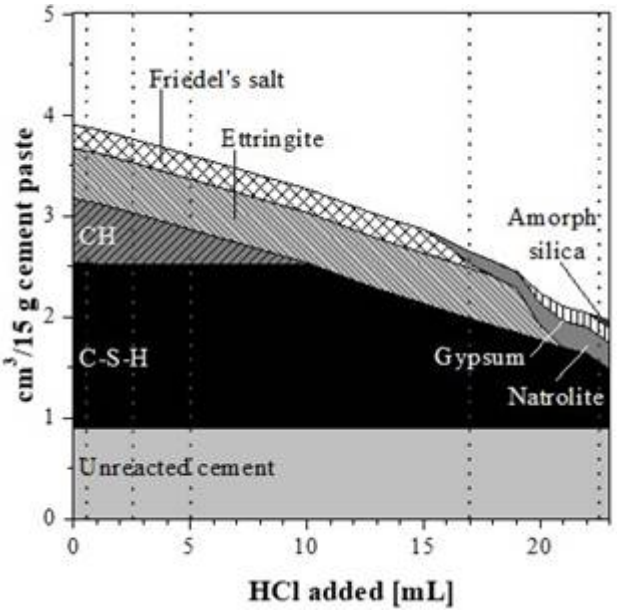

Figure 2 - The predicted changes in phase assemblage (in cm^3 / 15 g cement paste) upon the addition of increasing volumes of 4 mol/L HCl (in mL). The sample contained initially 15 g moist hydrated cement paste and 20 mL of 1.5 mol/L NaCl solution. The acid additions (0.5, 2.5, 5, 17, and 22.5 mL) which were used in this study are indicated by the dotted lines.

Figure 3 shows the predicted development of the pH of the exposure solution for increasing amounts of HCl added (pH GEMS - solid line) which corresponds to the modelling of the solid phase assemblage shown in Figure 2. The pH decreases steadily upon HCl addition, with a small plateau between approx. 5 and 10 mL acid addded. This is due to the presence of portlandite which buffers the pH. When portlandite is predicted to have dissolved, at around 10 mL HCl added, the pH drops further. In order to verify the predicted pH development experimentally, one sample was acidified (OPC 22.5) in steps of 0.25, 1 and 2 mL HCl until the sample tube was filled. The pH-values were measured both directly after adding acid (instant pH - triangles) and after 1-3 days of equilibration (pH at EQ - spheres). The experimentally obtained pH-development curves are also included in Figure 3. The measured pH and the modelled pH agree well.

The fact that there was hardly any difference in pH directly after adding acid and one day later when less than 7 mL acid was added in steps of 0.25 mL indicates that for these small additions the system rapidly reaches equilibrium, meaning there is no severe instantaneous drop in the pH of the solution. The risk of locally dissolving phases other than portlandite is therefore low. However, the difference between pH immediately after acid addition and after 1-3 days increased for higher additions, likely because of larger amounts acid were added per step combined with the lower buffer capacity of the system.

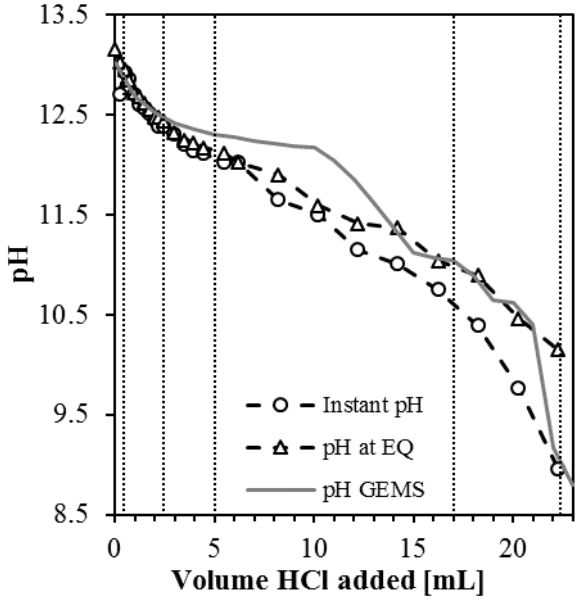

Figure 3 - Development of the pH of the exposure solution upon stepwise addition of HCl (4 mol/L). The sample contained initially 15 g moist hydrated cement paste and 20 mL of 1.5 mol/L NaCl solution. The values experimentally determined 10 min after acid addition, i.e. instant pH (spheres), the pH after 1-3 days of equilibration (triangles) and the pH predicted by thermodynamic modelling with GEMS (solid line) are compared. The acid additions (0.5, 2.5, 5, 17, and 22.5 mL) which were used in this study are indicated by the dotted lines.

Based on the measured pH and the predicted phase assemblage, four levels of acid addition were selected for further investigation: 0, 0.5, 2.5, 5 and 17 mL HCl. The levels are indicated in Figure 2 and Figure 3 with dotted lines. The sample without acid (OPC-0) is considered as a reference. At these acid additions, separate samples were prepared to investigate the chloride binding and the phase assemblage. The results of these investigations are reported in the

following sections. The 0.5, 2.5 and 5 mL additions were aimed to reflect different levels of moderate leaching as the system was predicted to still contain portlandite. The level of 17 mL would reflect advanced leaching as portlandite was nearly depleted and the main hydration phase C-S-H would start to decompose.

3,2 Chloride binding

Figure 4 a) and b) show the experimentally determined amount of bound chlorides for the samples as a function of the pH or the free chloride concentration in the liquid phase respectively. With increasing amounts of acid added (indicated by the arrows in both figures), the pH decreases and the free chloride concentration increases. When the pH drops from 13.2 to about 12.2 (≤5 mL of acid added), the amount of bound chlorides increased with decreasing pH and increasing free chloride concentration. At a pH of 11 (sample OPC-17) the cement paste showed close to no chloride binding. Figure 4 also shows the amount of bound chlorides as predicted by the thermodynamic model (dotted line). Friedel's salt is the only phase that is assumed to bind chlorides in the thermodynamic model, thus the model also predicts constant chloride binding in the range of 0-15 mL acid added (pH 13.2-11.1). At higher acid addition, Friedel's salt was predicted to decompose (see Figure 2) and consequently the amount of bound chlorides is predicted to drop to zero. Hence, the model can potentially account for the loss of binding capacity at a pH of 11, but not for the observed increase of chloride binding upon lowering the pH from 13.2 to about 12.2.

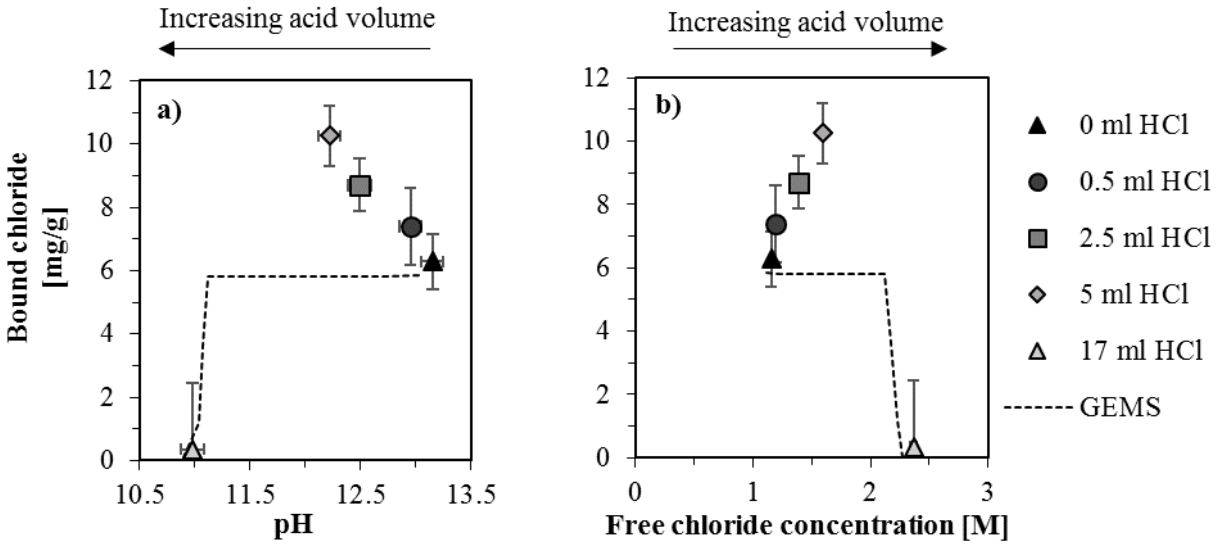

Figure 4 - Amount of bound chlorides in the ordinary Portland cement paste samples exposed to 1.5 mol/L NaCl solution to which varying amounts of HCl was added (0, 0.5, 2.5, 5 and 17 mL) as a function of a) the pH, and b) the free chloride concentration in the liquid phase at equilibrium. The symbols represent the experimentally determined bound chlorides and the dotted line the one predicted by the model. The error bars for the amount of bound chloride and the free chloride concentration were calculated with a Gaussian error propagation. The error of the pH determination was estimated to ± 0.1.

3.3 Phase assemblage

To elucidate the mechanisms that cause the changes in chloride binding described above, this section presents the investigation of the phase assemblage of the Portland cement paste samples

exposed to 1.5 mol/L NaCl solution to which 0, 0.5, 2.5, 5, 17 and 22.5 mL of HCl was added. The results are discussed and compared to the results of the thermodynamic modelling in the following.

Figure 5 presents the TGA-curves for all the chloride exposed samples and for OPC that has not been exposed to any chloride solutions (OPC-No Cl), as well as the derivative of the TGA-curves of these sample, the DTG curves. The typical weight loss peaks for ettringite (Et), C-S-H, monosulphate (Ms), monocarbonate (Mc), Friedel's salt (Fs), hydrotalcite (Ht), portlandite (CH) and carbonates are indicated.

Figure 6 shows the XRD-spectra of all samples in this study, including the reference, to which no HCl was added (OPC-0) in the range between 8.5-12° 2θ and 31-35° 2θ. The peak positions of ettringite (Et), Friedel's salt (Fs), portlandite (CH) and NaCl are indicated. Clear peaks of NaCl were observed in all samples exposed to a chloride solution. This indicates that the sample preparation for XRD was not able to remove the pore solution completely, which resulted in the precipitation of e.g. NaCl upon drying.

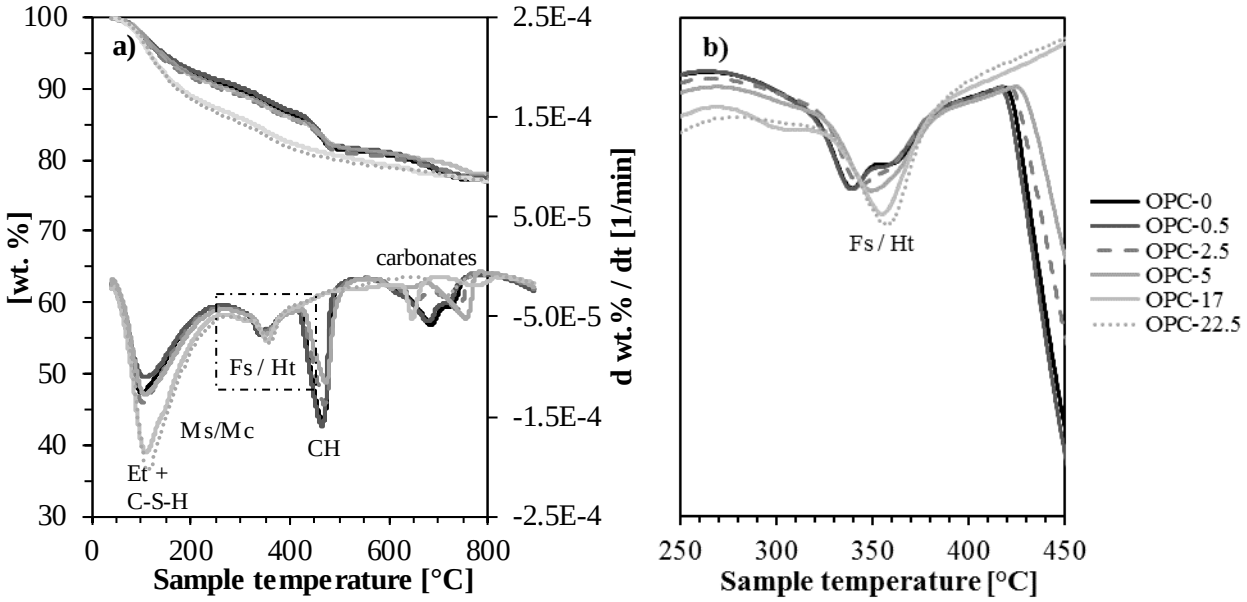

Figure 5 – a) TG (in wt. % of initial mass) and DTG (in wt. %/min) curves of the ordinary Portland cement (OPC) paste samples exposed to 1.5 mol/L NaCl solution to which varying amounts of HCl (4 mol/L) was added (0, 0.5, 2.5, 5, 17, and 22.5 mL). The typical weight loss peaks for ettringite (Et), C-S-H, monosulphate (Ms), monocarbonate (Mc), Friedel's salt (Fs), hydrotalcite (Ht), portlandite (CH) and carbonates are indicated. Figure 5 b) shows the DTG curves of all samples zoomed into the temperature range between 250 and 450°C as indicated by the rectangle in a).

Portlandite

A clear decrease in the portlandite weight loss peak near 450°C was observed with increasing acid additions (Figure 5). Moreover, the XRD peak for portlandite also appears to decrease with increasing additions of acid (Figure 6). The experimental results from TGA and XRD agree well with the thermodynamic model. The amount of portlandite in the samples for the various additions of acid predicted by the thermodynamic modelling (OPC-0: 19 wt%, OPC-5:

10wt%/10, OPC-17: 0 wt%) agree well with the experimentally obtained values with TGA (OPC-0: 15 wt%, OPC-5: 10 wt%, OPC-17: 0 wt%).

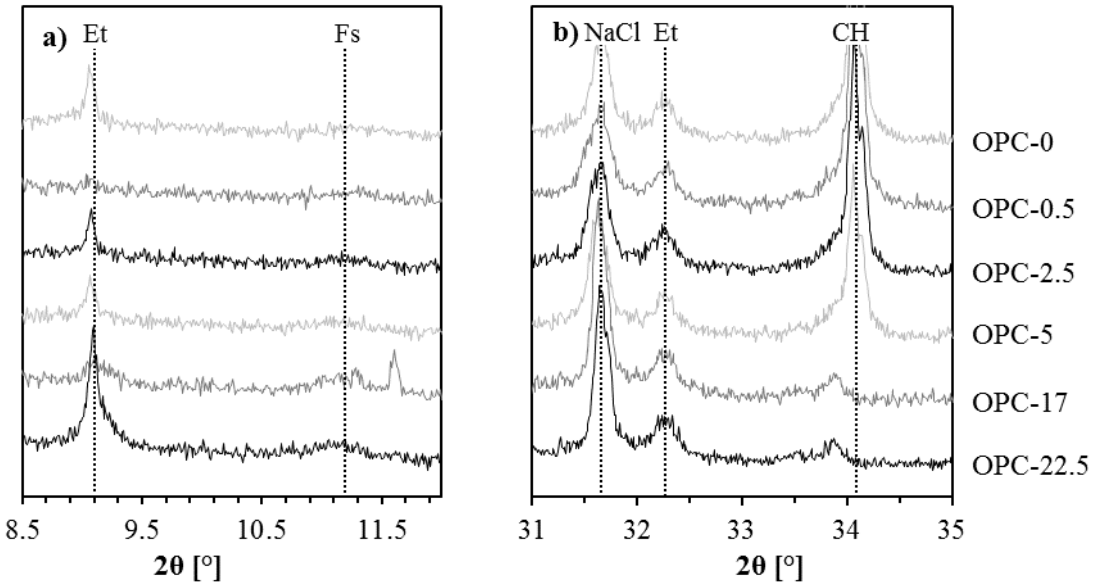

Figure 6 - XRD spectra of the ordinary Portland cement (OPC) paste samples exposed to 1.5 mol/L NaCl solution to which varying amounts of HCl was added (0, 0.5, 2.5, 5, 17 and 22.5 mL in the range between a) 8.5-12° 2θ and b) 31-35° 2θ. The peak positions of ettringite (Et), Friedel's salt (Fs), portlandite (CH) and NaCl are indicated.

AFm/AFt

The weight loss peak near 350°C showed a double peak for the samples to which no or only small amounts of acid were added (≤ 2.5 mL), which might indicate the formation of Friedel's salt in these samples [21]. As acid was added, the peak shape changed back to a single peak, as in samples to which no chlorides (NaCl) were added (not shown here). Neither the presence nor the decomposition of Friedel's salt could be verified by XRD as no characteristic reflection peaks for Friedel's salt were observed in any of the XRD spectra (Figure 6). There is a small hump in the spectra near 11.19° 2θ, which might indicate that the phase is present but is poorly crystalline. SEM-EDS did also not allow the detection of Friedel's salt, indicating that if it is present it is finely intermixed with the other hydrates.

The model predicts the presence of Friedel's salt in the chloride containing samples, and its decomposition for acid additions above 15 mL (Figure 2). Even though the model does not predict any changes in the amount of Friedel's salt for acid additions up to 15 mL, there are some slight changes in the DTG peaks related to the AFm phases upon acid addition up to 5 mL (Figure 5b). However, without clear XRD peaks of these phases their identification is not possible.

The absence of typical diffraction peaks for AFm phases such as Friedel's salt ($3CaO{\cdot}Al_2O_3{\cdot}CaCl_2{\cdot}10H_2O$, 11.19° 2θ), monocarbonate ($3CaO{\cdot}Al_2O_3{\cdot}CaCO_3{\cdot}11H_2O$, 11.7° 2θ) or monosulphate ($3CaO{\cdot}Al_2O_3{\cdot}CaSO_4{\cdot}11H_2O$, 10.3° 2θ) in the XRD-spectra is most likely related to the high curing temperature applied [28]. The paste was cured for 7 months at 60°C, before being stored at 20°C for more than 13 months. Ettringite is not stable at 60°C [28]. Lowering of the curing temperature afterwards might have caused delayed ettringite formation

[29]. The occurrence of delayed ettringite formation in the current study is supported by the distinct reflections for ettringite in the samples investigated (Figure 6). The only sample that did not show a clear reflection of ettringite is OPC-0.5. The reason for this is unknown. The presence of ettringite for HCl additions up to 19 mL was predicted by the thermodynamic model (Figure 2).

C-S-H

According to the thermodynamic model (Figure 2), C-S-H remains stable as long as there is portlandite present in the cement paste. The TGA results (Figure 5) might give the impression that more C-S-H is present in the heavily leached samples (OPC-17 and OPC-22.5), however this is not the case. This is due to the dissolution of portlandite, which is causing the weight loss peaks of all other non-dissolving phases to increase, as the results are expressed relative to the initial mass of the sample.

SEM-EDS was used to investigate changes in the C-S-H composition with increasing amounts of HCl added. SEM-EDS point analyses were taken in the matrix of the various samples. The results of these point analyses were plotted as the Al/Ca over the Si/Ca ratio. The Si/Ca ratio (and thereby the Ca/Si ratio) of the C-S-H was determined as described by Taylor [9]. Figure 7 shows the Ca/Si-ratio of the C-S-H as determined by EDS, and the predicted Ca/Si-ratio and volume of C-S-H in the GEMS model as a function of the pH of the exposure solution.

Figure 7 shows that there are changes in the Ca/Si ratio of the C-S-H even though its volume remains constant. The EDS data and the model both show that the Ca/Si ratio of the C-S-H slightly increased with decreasing pH (acid additions $\leq$ 5 mL). For acid additions larger than 5 mL (pH $\leq$ 11) the Ca/Si ratio decreased again. The sample OPC-22.5 showed with 1.2 a considerably lower Ca/Si ratio as the sample OPC-0 (Ca/Si = 1.4). According to the model, the decomposition of C-S-H starts at a pH of 12.6, at which point the Ca/Si-ratio also rapidly declines as the pH decreases. This indicates that for sample OPC-17 and OPC-22.5, it is possible that decomposition of the C-S-H has occurred.

The results from the EDS should be interpreted with care, as sample preparation might have caused an artificial increase in the calcium content due to precipitation from the exposure solution. However, similar trends of changed Ca/Si-ratio have been observed by De Weerdt and Justnes [30], who showed that in cement paste leached by sea water, C-S-H was decalcified from a Ca/Si-ratio of 1.8 down to 1.

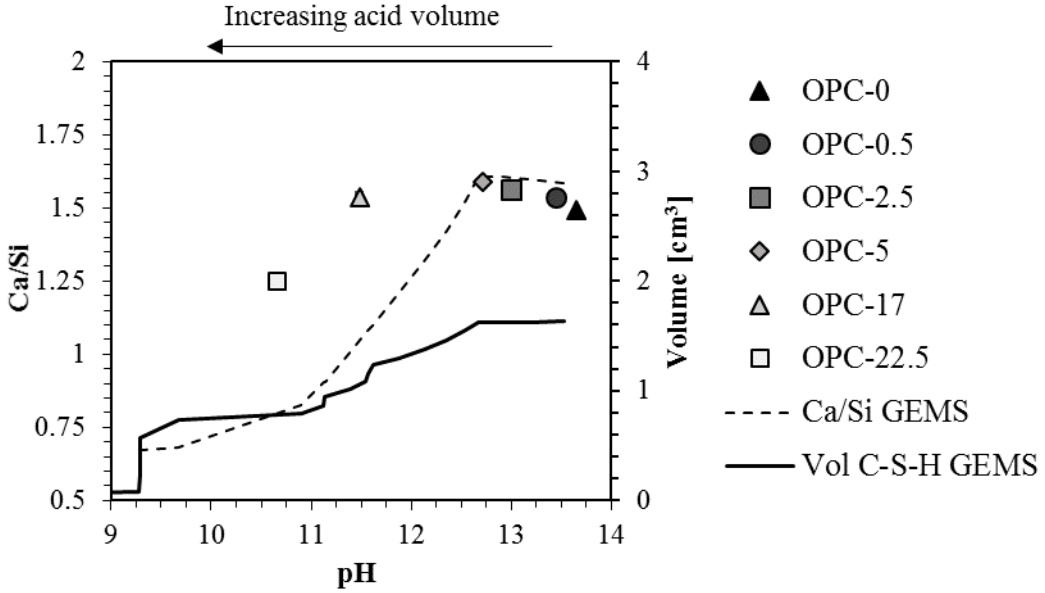

Figure 7 - Development of the Ca/Si ratio of the C-S-H as a function of the pH in the pore solution determined experimentally (symbols) and predicted by the thermodynamic modelling (dashed line). In addition, the predicted volume of C-S-H upon increasing amounts of acid as predicted by the thermodynamic modelling is shown.

Composition of the liquid phase

The symbols in Figure 8 show the concentrations of Ca, Cl, Na, K and S experimentally obtained with ICP-MS in the solution of the samples over a) the amount of acid added and b) the pH in the samples. The lines represent the concentration of the various elements in the pore solution as predicted by GEMS. There is a relatively good agreement between the measured and modelled results. The concentrations of Ca and Cl increase as acid is added, whilst the concentrations of Na and K decrease. The increase in Cl concentration is due to the addition of 4 mol/L HCl. The increase in the Ca-content is caused by the dissolution of portlandite and the decreased Ca/Si-ratio of the C-S-H. The gradual decrease in the Na and K concentrations are due to the dilution with acid. The concentration of S decreases initially, before increasing for the 17 ml acid sample and decreasing slightly from 17 to 22.5 ml. For S the initial decrease in concentration is likely due to dilution, whilst the eventual increase is caused by the dissolution of ettringite.

4. DISCUSSION ON THE ALTERED CHLORIDE BINDING DUE TO THE ARTIFICIAL LEACHING

4.1 Increase in chloride binding for acid additions ≤ 5 mL

Figure 9 combines the chloride binding results from this study (Figure 4b) with the chloride binding isotherms determined by Machner et al. [31] on samples with the same composition cured as well at 60°C and exposed at 20°C to either NaCl or $CaCl_2$ solutions. In the case of NaCl, the slope of the binding isotherm at free chloride concentrations above 1 mol/L increases only marginally and develops towards a plateau [31]. This means that increasing the chloride concentration above 1 mol/L should not contribute to considerably increased chloride binding.

However, upon the addition of HCl, the chloride binding increases more than could be explained by the increase in free chloride concentration.

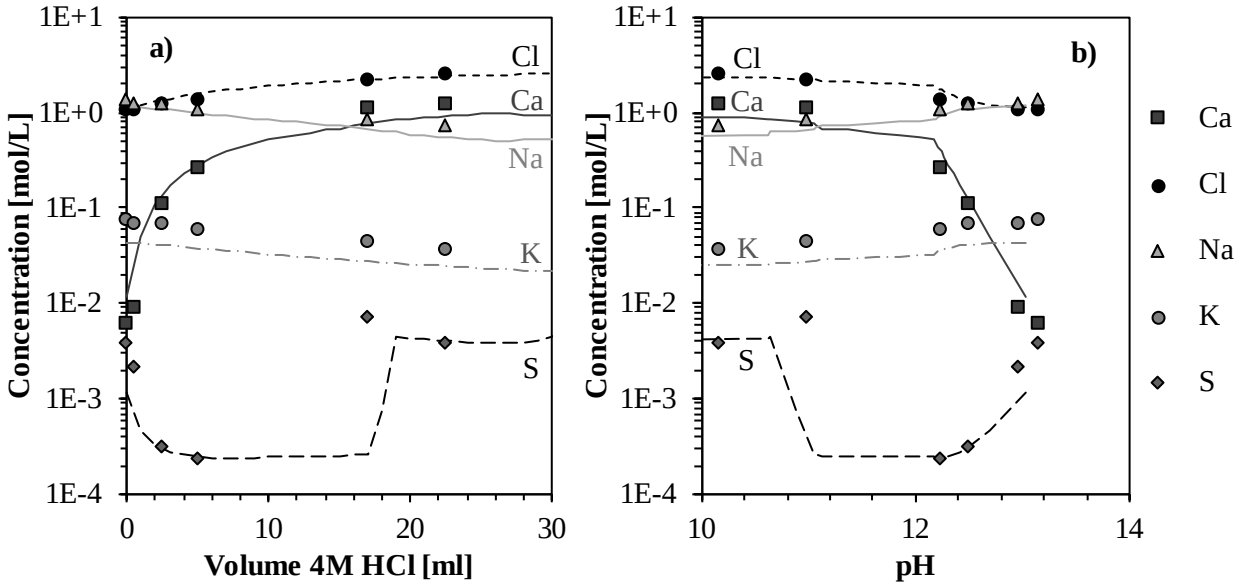

Figure 8: The measured (symbols) and modelled (lines) elemental concentrations in the solution of the samples as a function of a) the amount of acid added to each sample and b) the pH of the solutions.

The values of the bound chloride with HCl additions develop rather towards the values of the chloride-binding isotherm for $CaCl_2$ exposure reported previously [31]. Significantly greater chloride binding has been reported previously when samples were exposed to solutions of $CaCl_2$ rather than NaCl [13,16–20,32]. HCl has a similar effect on the system as $CaCl_2$, as both lower the pH and increase the calcium concentration, the former by dissolving portlandite and the latter by supplying additional calcium during its dissolution. The difference between the chloride-binding capacity of samples exposed to NaCl and $CaCl_2$ has been largely attributed to two different mechanisms.

Role of the Friedel's salt

Shi et al. [16] observed the formation of a larger amount of Friedel's salt in composite cement paste samples containing metakaolin exposed to $CaCl_2$ than in samples exposed to NaCl. He explained this by the additional calcium that is available in the case of $CaCl_2$ exposure. With the formation of larger amounts of Friedel's salt, more chloride ions are bound chemically and the chloride-binding capacity of the cement paste increased. However, no increase in the amount of Friedel's salt formed was observed for Portland cement pastes [16].

Whether the additional calcium in the pore solution due to the dissolution of the portlandite upon HCl addition lead to the formation of additional Friedel's salt could not be elucidated in this study. The high curing temperature (60°C) of the samples before exposure caused the AFm phases to be poorly crystalline, which made their identification with XRD impossible. For acid additions up to 5 mL, the thermodynamic modelling predicts the dissolution of portlandite and the changes in the Ca/Si ratio of the C-S-H fairly well. Therefore, the thermodynamic model should be able to predict additional Friedel's salt formation due to an increased calcium concentration in the pore solution. However, the model predicts a constant amount of Friedel's

salt to be present in samples to which less than 15 mL of HCl was added, which is within the range of acid additions that showed an increased chloride binding. This indicates that the increased chloride-binding capacity of the samples is probably not due to the formation of additional Friedel's salt.

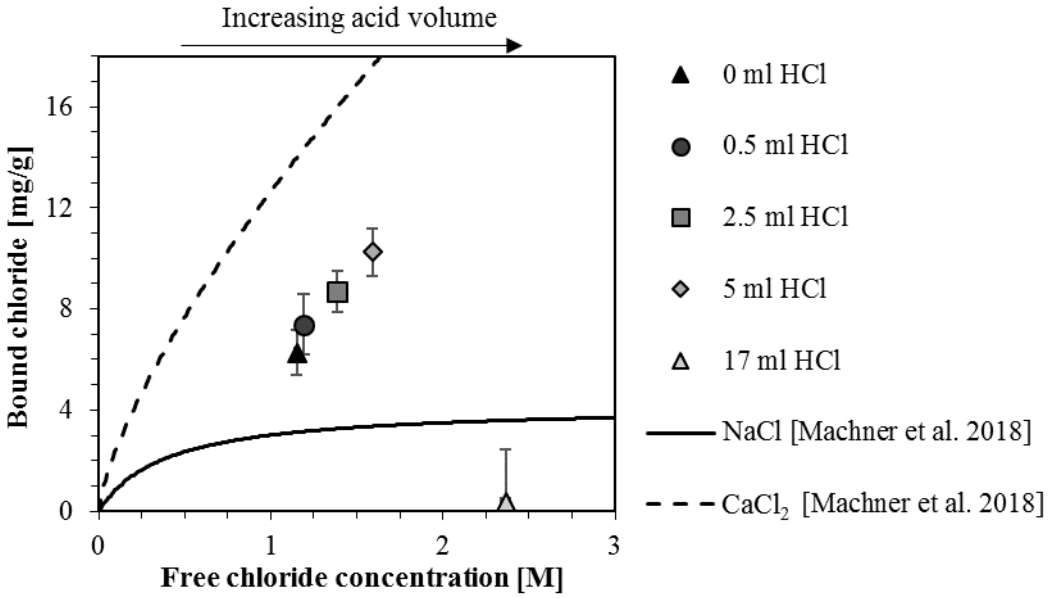

Figure 9 - Development of the amount of bound chlorides with increasing free chloride concentrations in the liquid phase of this study compared to previous results from Machner et al. [31].

Role of the C-S-H

The increased chloride-binding capacity of cement paste samples exposed to $CaCl_2$ compared to NaCl has also been explained by an increased amount of chlorides that can be accumulated in the diffuse layer of the C-S-H in the case of $CaCl_2$ exposure. This has previously been explained by the overcompensation of the originally negative surface charge of the C-S-H by the adsorption of divalent calcium ions in the Stern layer of the C-S-H [33]. This overcompensation reverses the surface charge and turns it positive [33], which means negatively charged chloride ions can accumulate in the diffuse layer of the C-S-H [19,34]. Such a reversal in the surface charge leading to the accumulation of chlorides in the diffuse layer has not been observed with monovalent ions, like Na^+ [19]. The exposure of cement pastes to $CaCl_2$ solutions has also been reported to be accompanied by a decrease in the pH of the pore solution and an increase in chloride binding [14,16–19].

The C-S-H in this study changed its Ca/Si ratio upon HCl addition (Figure 7). The changes in chloride binding could therefore be due to changes in accumulation of ions in the diffuse layer of C-S-H. As shown in Figure 4 the amount of bound chlorides increased with increasing amount of acid added up to 5 mL and consequently with decreasing pH from 13.2 to 12.2. With decreasing pH, more silanol groups are deprotonated (as schematically shown in Eq. (4), where > indicates the connection of the silanol group to the calcium layer), which leads to an increase in the negative surface charge density [35]. Consequently, more calcium ions from the pore solution can be adsorbed on the C-S-H in the Stern layer leading to a larger overcompensation of the surface charge [35]. This is visible in the increased Ca/Si ratio of the C-S-H for acid

additions ≤ 5 mL (Figure 7). This might consequently lead to a larger amount of chloride ions accumulated in the diffuse layer of the C-S-H. The dissolution of portlandite upon acid addition ensured sufficient calcium ions in the pore solution (Figure 8) to overcompensate the negative surface charge of the C-S-H.

$$> SiOH \rightarrow SiO^- + H^+ \quad (4)$$

Moreover, a decrease in the pH of the pore solution leads to a reduction of competing accumulation by hydroxyl ions, which might increase the accumulation of chloride ions in the diffuse layer additionally [14].

4.2 Decrease in the chloride-binding capacity for higher acid additions

The results of the chloride binding in this study also showed that when 17 mL of HCl was added the cement paste shows almost no chloride-binding capacity. This indicates that after a certain amount of acid has been added, the reduced pH in the pore solution caused the dissolution of chloride-binding phases or prevents them in other ways from binding chlorides.

When more than 5 mL of HCl has been added the C-S-H starts to decalcify, as shown by the Ca/Si ratio in Figure 7. This potentially renders the phase less positively charged, and reduces the accumulation of chloride in the diffuse layer. Additionally, the amount of C-S-H is predicted to decrease for pH values lower than 12.6 (less than 5 mL acid added). Both mechanisms are probably responsible for the decrease in the chloride-binding capacity of the paste samples at HCl additions of more than 5-10 mL. The loss of chloride binding in the outermost section of concrete due to extensive leaching has also been reported for field samples exposed to sea water [7,8] and exposed to NaCl solution [4].

4.3 Further work

The current study was performed as a proof of concept for an experimental setup that can be used to study the impact of the pH of the pore solution on the chloride binding of hydrated cement paste. For further work, the following remarks will be taken into account.

Due to the limited availability of cement paste and therefore the number of samples in the current study, the exact point at which the chloride binding decreases is unknown. If it continues to increase until it drops to zero or gradually declines will be investigated in a follow-up study.

Because the cement paste samples were cured at 60°C before they were exposed to NaCl solutions and HCl, the Friedel's salt in the paste was not crystalline and its contribution to the chloride binding could not be conclusively determined. In a follow-up study, cement paste samples cured at 20°C will be prepared and investigated using the methods developed here. This should lead to samples containing crystalline AFm phases and should make it possible to distinguish between the effects of AFm phase and C-S-H to the chloride binding of the cement paste.

Improvements should be made to the sample preparation for analysis of the solids. The current method of double solvent exchange and filtration appears to cause the precipitation of NaCl and potentially calcium from the pore solution, probably due to the inability of the used solvents

(isopropanol and petroleum ether) to penetrate the gel porosity of the C-S-H phase during the solvent exchange and replace the pore solution between the C-S-H sheets. This was explained by the big molecular size of alcohols compared to water, which inhibits the replacement of the water in very small pores [36]. This makes the solids analyses by XRD, SEM and TGA less representative. A possible solution could be "washing" the solids with a known amount of deionized water over a specified amount of time, similarly to the method described by Plusquellec et al. [37]. This would help to remove precipitates like NaCl before solvent exchange.

5. CONCLUSIONS

A method for lowering the pH of the pore solution in a hydrated cement paste in a closed system was developed.

Chloride binding of a hydrated cement paste was observed to be closely linked to the pH in the pore solution. Lowering the pH from 13.2 to 12.2 increases chloride binding. If the pH drops to 11, the chloride binding of the cement paste is greatly reduced.

The applied thermodynamic model indicates that the pH dependency of the chloride binding is connected to pH-dependent changes in the Ca/Si ratio of the C-S-H. The low crystallinity of the Friedel's salt in the investigated samples did not allow us the experimentally verify its role in the pH-dependent chloride binding.

These findings might explain why in concrete structures, harsh leaching at the surface will reduce the chloride binding, while moderate leaching further into the concrete leads to increased chloride binding and therefore an increased maximum in the chloride profile. In order to obtain more accurate chloride ingress predictions, service life prediction models for concrete structures exposed to chlorides should incorporate the effect of lowered pH due to leaching on chloride binding.

ACKNOWLDEGMENTS

The authors would like to thank Kjell Wiik (NTNU) for the cooperation within the Master Thesis project of Petter Hemstad, which resulted in this study. The authors would also like to thank Norcem AS for providing the cement used in this study. We are also very grateful for the helpful discussions on the chloride exposure and the C-S-H with Tone Østnor (SINTEF) and Gilles Plusquellec (RISE).

REFERENCES

1. Galan I & Glasser F P: "Chloride in cement," *Advances in Cement Research*, Vol. 27, 2015, pp. 63–97.
2. International Federation for Structural concrete, *fib*, Model Code for Service Life Design: Model code prepared by Task group 5.6, fib, Lausanne, 2006.
3. Fick A, "Über Diffusion," *Annalen der Physik*, Vol. 170, 1855, pp. 59–86.

4. De Weerdt K, Lothenbach B & Geiker M R: "Comparing chloride ingress from sea water and NaCl solution in Portland cement mortar," Submitted for publication to *Cement and Concrete Research*, April, 2018.
5. De Weerdt K, Justnes H, Geiker M R: "Changes in the phase assemblage of concrete exposed to sea water," *Cement and Concrete Composites*, Vol. 47, 2014, pp. 53–63.
6. Geiker M R: "Fly ash in concrete, Danish experience," 2015. *Report* No. 370, Norwegian Public Roads Administration, Oslo, Norway.
7. Jakobsen U H, De Weerdt K & Geiker M R: "Elemental zonation in marine concrete," *Cement and Concrete Research*, Vol. 85, 2016, pp. 12–27.
8. De Weerdt K, Orsáková D, Muller A C A, Larsen C K, Pedersen B, Geiker M R: "Towards the understanding of chloride profiles in marine exposed concrete, impact of leaching and moisture content," *Construction and Building Materials*, Vol. 120, 2016, pp. 418–431.
9. Taylor H F W: Cement Chemistry, 2nd ed., Telford, London, UK, 1997.
10. Justnes H: "A Review of Chloride Binding in Cementitious Systems," *Nordic Concrete Research*, Vol. 21, 199, pp. 48-63.
11. Roberts M H: "Effect of calcium chloride on the durability of pre-tensioned wire in prestressed concrete," *Magazine of Concrete Research*, Vol. 14, 1962, pp. 143–154.
12. Suryavanshi A K, Narayan Swamy R: "Stability of Friedel's salt in carbonated concrete structural elements," *Cement Concrete Research*, Vol. 26, 1996, pp. 729–741.
13. Arya C, Buenfeld N R, Newman J: "Factors influencing chloride-binding in concrete," *Cement Concrete Research*, Vol. 20, 1990, pp. 291–300.
14. Tritthart J: "Chloride binding in cement - II. The influence of the hydroxide concentration in the pore solution of hardened cement paste on chloride binding," *Cement Concrete Research*, Vol. 19, 1989, pp. 683–691.
15. Hansson C M, Frølund T, Markussen JB: "The effect of chloride cation type on the corrosion of steel in concrete by chloride salts," *Cement Concrete Research*, Vol. 15, 1985, pp. 65–73.
16. Shi Z, Geiker MR, De Weerdt K, Østnor TA, Lothenbach B, Winnefeld F & Skibsted J: "Role of calcium on chloride binding in hydrated Portland cement–metakaolin–limestone blends," *Cement Concrete Research*, Vol. 95, 2017, pp. 205–216.
17. Zhu Q, Jiang L, Chen Y, Xu J, Mo L: "Effect of chloride salt type on chloride binding behavior of concrete," *Construction Building Materials*, Vol. 37, 2012, pp. 512–517.
18. De Weerdt K, Colombo A, Coppola L, Justnes H, Geiker MR: "Impact of the associated cation on chloride binding of Portland cement paste," *Cement Concrete Research*, Vol. 68, 2015, pp. 196–202.
19. Wowra O, Setzer MJ: "Sorption of chlorides on hydrated cement and C_3S pastes," in: M.J. Setzer, R. Auberg - Eds., Frost Resistance of Concrete, E & FN Spon, London, UK, 1997, pp. 147–153.
20. De Weerdt K, Orsáková D, Geiker M:"The impact of sulphate and magnesium on chloride binding in Portland cement paste," *Cement Concrete Research*, Vol. 65, 2014, pp. 30–40.
21. Lothenbach B, Durdzinski P, De Weerdt : "Thermogravimetric Analysis," in: Scrivener K, Snellings R, Lothenbach B- Eds., A Practical Guide to Microstructural Analysis of Cementitious Materials, CRC Press Taylor & Francis Group, Raton, 2015, pp. 177–211.
22. Kulik D: GEM-Selektor v.3.3, available at: http://gems.web.psi.ch/.

23. Kulik D, Wagner T, Dmytrieva S, Kosakowski G, Hingerl FF, Chudnenko KV, Berner UR: GEM-Selektor geochemical modeling package: Revised algorithm and GEMS3K numerical kernel for coupled simulation codes, *Computer and Geoscience*, Vol. 17, 2013, pp. 1–24.
24. Wagner T, Kulik D, Hingerl F, Dmytrieva SV: "GEM-Selektor geochemical modeling package: TSolMod library and data interface for multicomponent phase models, " *The Canadian Mineralogist*, Vol. 50, 2012, pp. 1173–1195.
25. Thermodynamic database, provided by EMPA, available at: https://www.empa.ch/web/s308/thermodynamic-data.
26. Kulik D: "Improving the structural consistency of C-S-H solid solution thermodynamic models," *Cement Concrete Research*, Vol. 41, 2011, pp. 477–495.
27. Hemstad P: "pH-dependency of chloride binding in ordinary Portland cement." Master Thesis, Trondheim, Norway, 2018.
28. Lothenbach B, Winnefeld F, Alder C, Wieland E, Lunk P: "Effect of temperature on the pore solution, microstructure and hydration products of Portland cement pastes," *Cement Concrete Research*, Vol. 37, 2007, pp. 483–491.
29. Scrivener K, Taylor HFW: "Delayed ettringite formation: a microstructural and microanalytical study," *Advances in Cement Research*, Vol. 5, 1993, pp. 139–146.
30. De Weerdt K, Justnes H: "The effect of sea water on the phase assemblage of hydrated cement paste," *Cement and Concrete Composites*, Vol. 55, 2015, pp. 215–222.
31. Machner A, Zajac M, Ben Haha M, Kjellsen KO, Geiker MR, De Weerdt K: "Chloride-binding capacity of hydrotalcite in cement pastes containing dolomite and metakaolin," *Cement Concrete Research* , Vol. 107, 2018, pp. 163–181.
32. Delagrave A, Marchand J, Ollivier J-P, Julien S, Hazrati K: "Chloride Binding Capacity of Various Hydrated Cement Paste Systems," *Advanced Cement Based Materials*, Vol. 6, 1997, pp. 28–35.
33. Labbez C, Nonat A, Pochard I, Jönsson B, "Experimental and theoretical evidence of overcharging of calcium silicate hydrate," *Journal of Colloid and Interface Science*, Vol. 309, 2007, pp. 303–307.
34. Plusquellec G, Nonat A: "Interactions between calcium silicate hydrate, C-S-H, and calcium chloride, bromide and nitrate," *Cement Concrete Research*, Vol. 90, 2016, pp. 89–96.
35. Haas J, "Etude expérimentale et modélisation thermodynamique du système CaO-SiO_2-(Al_2O_3)-H_2O," *PhD thesis*, Université de Bourgogne, Dijon, France, 2012.
36. Zhang J, Scherer GW: "Comparison of methods for arresting hydration of cement," *Cement Concrete Research*, Vol. 41 ,2011, pp. 1024–1036.
37. Plusquellec G, Geiker M, Lindgård J, Duchesne J, Fournier B, De Weerdt K: "Determination of the pH and the free alkali metal content in the pore solution of concrete," *Cement Concrete Research*, Vol. 96 , 2017, pp. 13–26.